Transient Receptor Potential Channel Vanilloid 1 Contributes to Facial Mechanical Hypersensitivity in a Mouse Model of Atopic Asthma

曹, 愛琳

Lab Invest 103 (2023) 100149

LABORATORY INVESTIGATION

journal homepage: https://laboratoryinvestigation.org/

Research Article

Transient Receptor Potential Channel Vanilloid 1 Contributes to Facial Mechanical Hypersensitivity in a Mouse Model of Atopic Asthma

Ailin Cao[a,b], Weiqi Gao[a], Takeshi Sawada[a], Reiko U. Yoshimoto[a,b], Reona Aijima[c], Yasuyoshi Ohsaki[a], Mizuho A. Kido[a,b,*]

[a] *Division of Histology and Neuroanatomy, Department of Anatomy and Physiology, Faculty of Medicine, Saga University, Saga, Japan;* [b] *Department of Oral Pathology, Graduate School of Dental Science, Kyushu University, Fukuoka, Japan;* [c] *Department of Oral Maxillofacial Surgery, Faculty of Medicine, Saga University, Saga, Japan*

ARTICLE INFO

Article history:
Received 15 November 2022
Revised 22 March 2023
Accepted 29 March 2023

Keywords:
actin
allergy
glia
tactile allodynia
transient receptor potential channel
trigeminal ganglion

ABSTRACT

Sensitive skin, a common pathophysiological feature of allergic diseases, is defined as an unpleasant sensation in response to stimuli that normally should not provoke such sensations. However, the relationship between allergic inflammation and hypersensitive skin in the trigeminal system remains to be elucidated. To explore whether bronchial allergic inflammation affects facial skin and primary sensory neurons, we used an ovalbumin (OVA)–induced asthma mouse model. Significant mechanical hypersensitivity was observed in the facial skin of mice with pulmonary inflammation induced by OVA sensitization compared to mice treated with adjuvant or vehicle as controls. The skin of OVA-treated mice showed an increased number of nerve fibers, especially rich intraepithelial nerves, compared to controls. Transient receptor potential channel vanilloid 1 (TRPV1)–immunoreactive nerves were enriched in the skin of OVA-treated mice. Moreover, epithelial TRPV1 expression was higher in OVA-treated mice than in controls. Trigeminal ganglia of OVA-treated mice displayed larger numbers of activated microglia/macrophages and satellite glia. In addition, more TRPV1 immunoreactive neurons were found in the trigeminal ganglia of OVA-treated mice than in controls. Mechanical hypersensitivity was suppressed in OVA-treated *Trpv1*-deficient mice, while topical skin application of a TRPV1 antagonist before behavioral testing reduced the reaction induced by mechanical stimulation. Our findings reveal that mice with allergic inflammation of the bronchi had mechanical hypersensitivity in the facial skin that may have resulted from TRPV1-mediated neuronal plasticity and glial activation in the trigeminal ganglion.

Introduction

The skin provides important details about the external environment and initiates complex behavioral and emotional responses to mechanical, thermal, actinic, osmotic, and chemical stimuli. These stimuli activate specific receptors to produce a signal transduced by skin epithelial cells and sensory neurons innervating the skin, the cell bodies located in the trigeminal ganglion, and dorsal root ganglia (DRG).[1] Following proper detection and identification of innocuous and noxious stimuli in the skin, signals are relayed to neurons to maintain tissue barrier integrity and homeostasis of the body.[2] However, skin hypersensitivity, described as sensitive or reactive skin, is a common complaint of the general population globally.[3] Sensitive skin is defined by the occurrence of unpleasant sensations in response

* Corresponding author.
E-mail address: kido@cc.saga-u.ac.jp (M.A. Kido).

https://doi.org/10.1016/j.labinv.2023.100149

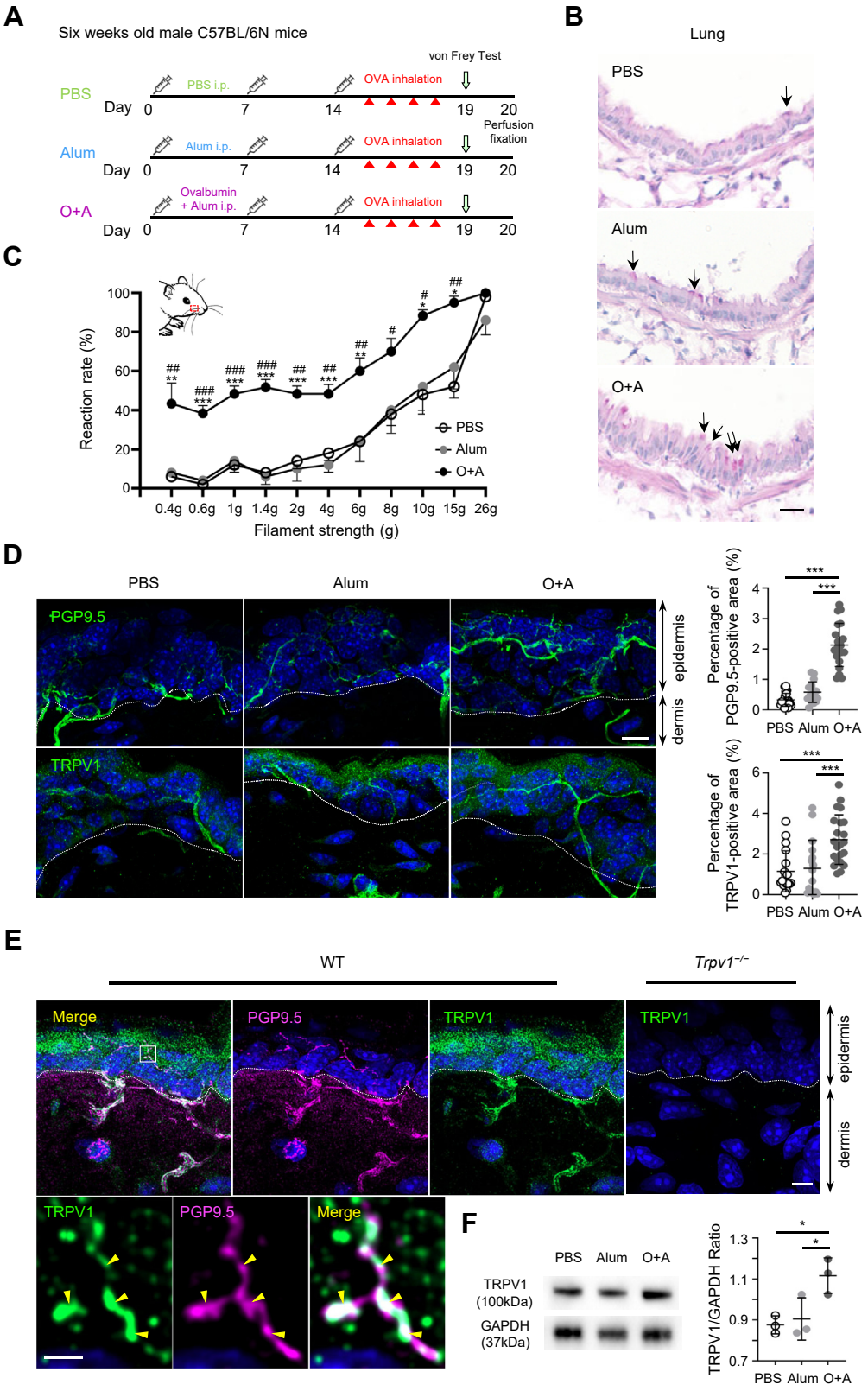

Figure 1.
Mechanical hypersensitivity of facial skin in the mouse model of atopic asthma. (A) Schematic of an atopic asthma mouse model. (B) Epithelial hyperplasia with goblet cells is indicated by PAS-positive mucous polysaccharide and a thickened smooth muscle layer in the bronchus of O+A group mice compared with PBS or Alum groups. Scale bar = 20 μm. (C) Orofacial tactile allodynia was determined as reaction rates in a von Frey filament test with different stimulation strengths. The reaction rate was significantly higher in the O+A group than in the PBS and Alum groups. n = 5, 5, and 6, respectively. #$P < .05$; ##$P < .01$; ###$P < .001$. *$P < .05$; **$P < .01$; ***$P < .001$. #: PBS vs O+A. *: Alum vs O+A. (D) Representative immunofluorescence images of staining for PGP9.5 (a pan-neuronal marker) and TRPV1 in facial skin from PBS, Alum, and O+A groups. Note that the rich

to stimuli that normally should not elicit such perception and cannot be explained by lesions attributable to any skin disease.[4] Survey data on the prevalence of self-declared sensitive skin in various demographics showed that 60% to 70% of women and 50% to 60% of men have some degree of sensitive skin.[5] This hyperreactivity affects the quality of life of patients and can lead to the development of neuropsychiatric conditions. Accordingly, unpleasant sensations such as burning, stinging, tingling, pricking, tightness, dryness, or itching in response to various normally innocuous physical, chemical, and/or thermal stimuli have a substantial impact on affected individuals, society, and the health care system.

Allergic diseases such as atopic dermatitis and atopic asthma have become prevalent worldwide. Moreover, the number of patients with atopic diseases is reportedly increasing.[6] Sensitive skin is a common pathophysiological feature, especially in patients with atopic diseases.[7] Some patients with preceding severe atopic inflammation displayed multifocally affected central and peripheral nervous system tissues, termed atopic myelitis.[8] Patients with atopic myelitis have hyperIgEemia and characteristically report subjective unpleasant sensation or allodynia, even without spinal lesions.[9] Understanding of allergic skin inflammation and itch or pain from immunopathological and neurologic aspects has greatly progressed in recent years. However, the molecular and cellular mechanisms of unpleasant subjective sensory effects, such as mechanical hypersensitivity, remain to be elucidated.

The responsiveness to mechanical, chemical, or thermal stimuli is dependent on the specific sensitivity to the different stimulus modalities. Recently, members of the nonselective cation channel family, transient receptor potential (TRP) vanilloid 1 (TRPV1) and ankyrin 1 (TRPA1), were shown to be important neuronal or nonneuronal targets for allergic diseases such as hypersensitivity for rhinitis,[10] allergic keratoconjunctivitis,[11] or asthma.[12] Accumulating evidence has revealed the multiple pathophysiological roles of TRPV1 and TRPA1 in atopic diseases.[13,14] However, the involvement of these ion channels in hypersensitivity needs to be defined further.

Sensitive skin can affect all locations in the body, especially the face.[4] The facial sensation is conveyed by the trigeminal sensory afferent, the cell bodies of which are located in the trigeminal ganglion. Extensive studies have demonstrated that mechanisms underlying ectopic orofacial hypersensitivity are associated with trigeminal nerve injury or orofacial inflammation, and the trigeminal system is distinct from the spinal system.[15] However, because most of these studies used direct topical nerve transection, such as maxillary nerve or facial adjuvant injections,[16,17] it is unknown whether systemic allergic inflammation affects facial hypersensitivity.

To explore whether facial skin sensitivity is affected by systemic allergic conditions, we employed the ovalbumin (OVA) asthma mouse model to induce a Th2-directed allergic response. Here, we describe facial mechanical hypersensitivity in a mouse model whose hypersensitive behavior was mediated by transient receptor potential channel vanilloid 1 (TRPV1) in activated glia and neurons of the trigeminal ganglion.

Materials and Methods

Mice

Male C57BL/6N mice (19-24 g; Japan SLC Inc), *Trpv1*$^{-/-}$ mice,[18] and *Trpv1*$^{-/-}$*Trpa1*$^{-/-}$ mice[19] were used. *Trpv1*$^{-/-}$ and *Trpv1*$^{-/-}$*Trpa1*$^{-/-}$ mice were provided as a kind gift by Prof. M. Tominaga (Department of Physiological Sciences, Graduate University for Advanced Studies, Okazaki, Japan). Animals were housed in a temperature-controlled room (12-hour light-dark cycle) with free access to food and water. All experimental protocols were approved by Saga University (29-05-1) and Kyushu University (A27-167-0) Animal Care and Use Committees.

Atopic Asthma Mouse Model

An atopic asthma model mouse was generated as previously described.[20] Briefly, 6-week-old male mice were lightly anesthetized with 2% isoflurane (099-06571, Wako Pure Chemical Corporation), and intraperitoneally administered 50 μg of OVA (A5503, Sigma-Aldrich) and 2 μL of aluminum hydroxide hydrate gel suspension (Alum; LG-6000, Cosmo Bio Co Ltd) dissolved in 200 μL of phosphate-buffered saline (PBS) at days 0, 7, and 14 (O+A group). Mice intraperitoneally injected with PBS (PBS group) or Alum (Alum group) were used as controls. At day 14, the mice were lightly anesthetized with 2% isoflurane and intranasally challenged with OVA solution (2.5 mg/mL) for 4 consecutive days. On day 19, von Frey testing of the facial region was performed in all 3 groups (Fig. 1A).

Von Frey Test

Mechanical stimuli were applied to the whisker pad skin using von Frey filaments (0.4-26 g; Aesthesio, DanMic Global). Briefly, mice were lightly anesthetized with 2% isoflurane, placed in a restraint device,[21] and acclimated for 30 minutes in the test environment. The von Frey filament was presented perpendicular to the whisker pad skin with sufficient force to cause slight buckling against the skin and held for 2 to 3 seconds. Stimuli were presented at intervals of >10 s. The positive reaction was defined as face withdrawal. Each filament was tested 10 times, and the number of positive responses multiplied by 10 was recorded as the percent response.[22] The experimenter was blinded to the experimental condition and mouse genotype while performing these experiments.

Administration of the transient receptor potential channel vanilloid 1 antagonist

The TRPV1 antagonist N-(3-methoxyphenyl)-4-chlorocinnamanilide (SB366791; 472981-92-3, Sigma-Aldrich) was dissolved in dimethyl sulfoxide (dimethyl sulfoxide; final concentration of 1.25%) and diluted in 0.9% NaCl solution. Five

nerve bundles and intense intraepithelial nerves are positive for PGP9.5 and TRPV1. Epithelial TRPV1 immunoreactivity was prominent in the O+A group. Scale bar = 10 μm. Quantification of PGP9.5- and TRPV1-positive areas in the epidermis of facial skin from PBS, Alum, and O+A groups, respectively. n = 3 for each group. (E) Representative immunofluorescent superresolution images of TRPV1 (green) and PGP9.5 (magenta) facial skin from wild type and *Trpv1*$^{-/-}$ mice with an orthogonal projection of 15.68 μm. Scale bar = 5 μm. Lower panels show magnified 0.48-μm-thick orthogonal-projection images of the intraepithelial nerve, indicated by the white box in the upper panel. TRPV1 fibers colocalized to PGP9.5 (yellow arrowheads). Scale bar = 1 μm. (D, E) Airyscan superresolution microscopy. (E) Processed with Airyscan joint deconvolution. (F) Immunoblot analysis for TRPV1 in facial skin extracts of PBS, Alum, and O+A groups. n = 3 for each group. *$P < .05$; **$P < .01$; ***$P < .001$. Alum, aluminum hydroxide hydrate gel suspension; PAS, Periodic acid-Schiff; PBS, phosphate-buffered saline.

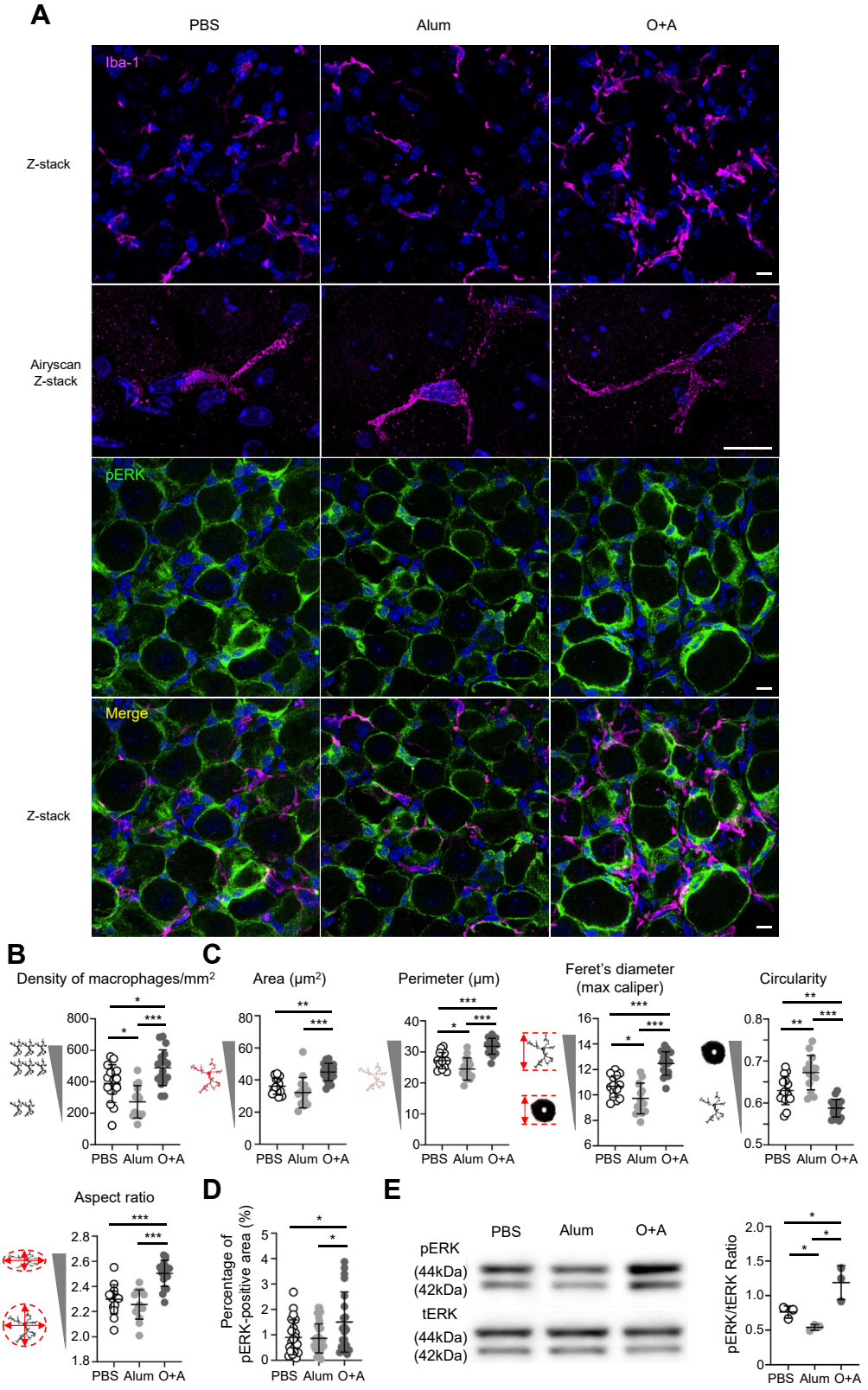

Figure 2.

Macrophage/microglial and satellite glial activation in the trigeminal ganglia of the atopic asthma mouse model. (A) Representative immunofluorescence images of staining for Iba-1 (a marker of microglia or macrophages; in magenta) and phosphorylated extracellular signal-regulated kinase (pERK; in green) in trigeminal ganglia from PBS, Alum, and O+A groups. Airyscan superresolution images of Iba-1 (second panel) were processed with an orthogonal projection of 6.56 μm. Images of the uppermost, third, and fourth panels were acquired by BC43. Uppermost and merged images in 10.9-μm z-stack. pERK images showing a single optical slice. Scale bar = 10 μm. (B) Quantitative analysis of microglial cell densities in trigeminal ganglia from PBS, Alum, and O+A groups. (C) Morphometric analysis of the shape characteristics of a single Iba-1-immunoreactive

micrograms of SB366791 or vehicle was injected into the facial skin of atopic asthma mice in a 20-μL volume using a 30-gauge needle in reference to previous reports.[17,23] The von Frey test was performed 30 minutes after facial injection of SB366791 or vehicle.

Immunohistochemical analyses

The day after von Frey testing, mice were anesthetized with a mixture of midazolam (4 mg/kg, 042824; Maruishi), butorphanol tartrate (5 mg/kg, VETLI5; Meiji Seika Pharma), and hydrochloric acid medetomidine (0.3 mg/kg, 9021; Kyoritsu Seiyaku), and then transcardially perfused with PBS containing sodium heparin (16H06; Nipro) and hydrochloride procaine (73091; Maruishi), followed by 4% paraformaldehyde (PFA; 104005; Merck KGaA) in pH7.4 phosphate buffer.

Subsequently, the skin and trigeminal ganglion were removed, postfixed in the 4% PFA overnight at 4 °C, cryoprotected by 20% sucrose (196-00015, Wako) overnight at 4 °C, and then embedded in OCT compound (4583; Sakura Finetek). All tissue sections were cut with a cryostat (Thermo Fisher Scientific). Trigeminal ganglion sections (10- or 20-μm-thick) and skin sections (30-μm-thick) were processed for immunohistochemistry according to our previous reports.[24] Sections were permeabilized with 0.3% Triton-X100 (203-03215, Wako) in PBS for 10 minutes at room temperature and then blocked in PBS with 1% bovine serum albumin (BSA; 10735078001; Roche), 0.05% sodium azide (NaN_3; 195-11092, Wako), and 5% normal donkey serum (NDS; 017-000-121, Jackson ImmunoResearch Laboratories) for 45 minutes. For staining with the mouse antibody, sections were processed with Mouse-on-Mouse (M.O.M.) mouse Ig blocking reagent (BMK-2202, Vector Laboratories) for 1 hour. Subsequently, sections were incubated overnight at 4 °C with the following primary antibodies: TRPV1 (rabbit, 1:10000),[25] ionized calcium-binding adapter molecule 1 (Iba-1; rabbit, 1:200; 019-19741, Wako), Iba-1 (goat, 1:200; ab5076; Abcam), protein gene product 9.5 (PGP9.5; rabbit, 1:2000; RA95101; Ultraclone), PGP9.5 (mouse, 1:400; 31A3; Ultraclone) calcitonin gene-related peptide (CGRP; rabbit, 1:2000; RPN1842; Amersham International), phospho-p44/42 MAPK (Erk1/2) (pERK; rabbit, 1:200; 9101; Cell Signaling Technology), and S100β (rabbit, 1:200; ab52642, Abcam). Next, sections were incubated for 1 hour at room temperature with the following secondary antibodies: donkey anti-rabbit IgG-Alexa488 (1:200; 711-545-152; Jackson ImmunoResearch Laboratories), donkey anti-goat IgG-Alexa546 (1:400; A11056; Invitrogen), and donkey antimouse IgG H&L (DyLight 649; 1:400; ab96878; Abcam). F-actin was visualized with Phalloidin-iFluor 647 Reagent (1:2000; ab176759, Abcam). Finally, the sections were incubated with 4',6-diamidino-2-phenylindole and dihydrochloride (DAPI; 1:1000; 340-07971; Dojindo Laboratories) for 5 minutes and then mounted with PermaFluor (TA-030-FM, Thermo Fisher Scientific). Images were acquired with laser confocal microscopies, BC43 (Oxford Instruments), or an LSM800 equipped with Airyscan (Carl Zeiss). Airyscan images were processed automatically determined superresolution parameters plus 0.5 additional manual adjustments per channel using ZEN Blue 3.5 (Carl Zeiss). In Figure 1E, 5 iterations of Airyscan joint deconvolution were used for excitations at 405 nm and 488 nm, and 8 iterations were used for excitations at 640 nm[26] using ZEN Blue 3.5. To correct for chromatic aberration, images of 0.2-μm TetraSpeck Microspheres (Thermo Fisher Scientific) loaded with 4 fluorescent dyes were taken as a reference in the same setting as the tissue samples. The registration and alignment of each channel were performed using the microsphere data and the "Channel Alignment (Extended)" tool in ZEN Blue 3.5.

Morphometric analysis of Iba-1–immunoreactive cells[27] and quantitative analyses of pERK- and F-actin–positive areas in trigeminal ganglia were performed with ImageJ software (National Institutes of Health). Quantitative immunoreactivity analyses of TRPV1 and CGRP neurons in trigeminal ganglia were performed by Lumina Vision 2.0 (Mitani Corporation). Cross-sectional areas of neuronal cell bodies with DAPI-labeled nuclei were analyzed from 12 sections per mouse. The proportions of TRPV1- and CGRP-positive neurons to total neuronal cell bodies in the trigeminal ganglion were analyzed. Morphometric analyses of the intraepithelial nervous distribution of PGP9.5, TRPV1, and CGRP in skin were analyzed with ImageJ software. The epithelial layer was manually selected as the region of interest in sections multicolor-stained for E-cadherin and DAPI, and areas immunopositive for PGP9.5, TRPV1, and CGRP were analyzed.

Periodic Acid-Schiff Staining

Lung tissues were removed and postfixed overnight at 4 °C in 4% PFA, cryoprotected by 20% sucrose overnight, and then embedded in OCT compound for sectioning in a cryostat at a 5-μm thickness. Periodic acid-Schiff (PAS)–stained sections were observed under an AxioImager2 microscope with ApoTome.2 (Carl Zeiss).

Immunoblot Analysis

Immunoblot analysis was performed as described previously.[28] Skin and trigeminal ganglia were collected and homogenized in lysis buffer (50 mM Tris-HCl, 150 mM NaCl, 1% Triton X-100, 0.5% NP-40) containing a protease inhibitor (Nacalai Tesque) and a phosphatase inhibitor cocktail (PhosSTOP; 04906845001, Roche) for 10 minutes on ice. Supernatants were collected, and the protein concentration was quantified with a Pierce BCA Protein Assay Kit (23225, Thermo Fisher Scientific). Protein extracts were separated by sodium dodecyl sulfate polyacrylamide gel electrophoresis and transferred to a polyvinylidene fluoride membrane. The membrane was blocked with 4% BSA for 1 hour at room temperature and then incubated overnight at 4 °C with the following primary antibodies: TRPV1 (rabbit, 1:4000), p44/42 MAPK (Erk1/2 [ERK]; rabbit, 1:4000; 9102; Cell Signaling Technology), pERK (rabbit, 1:4000; 9101; Cell Signaling Technology), TATA-binding protein (rabbit, 1:1000; 8515, Cell Signaling Technology), and glyceraldehyde-3-phosphate dehydrogenase protein (GAPDH; rabbit, 1:2000; sc25778, Santa Cruz Biotechnology). Specific bands were visualized using an ECL Prime Western Blotting Detection Reagent (RPN2232; GE Healthcare) and analyzed using a FUSION-FX7 imaging system (Vilber).

macrophage/microglia, including area, perimeter, circularity [$4\pi \times (\text{area}/\text{perimeter}^2)$], and Feret's diameter (max caliper). Aspect ratio is calculated as the ratio between the major and minor axis. (D) Quantification of pERK-positive area in the trigeminal ganglia. (E) Immunoblot analysis of pERK in trigeminal ganglia from PBS, Alum, and O+A groups. n = 3 for each group. *$P < .05$; **$P < .01$; ***$P < .001$. Alum, aluminum hydroxide hydrate gel suspension; PBS, phosphate-buffered saline; pERK, phospho-p44/42 MAPK.

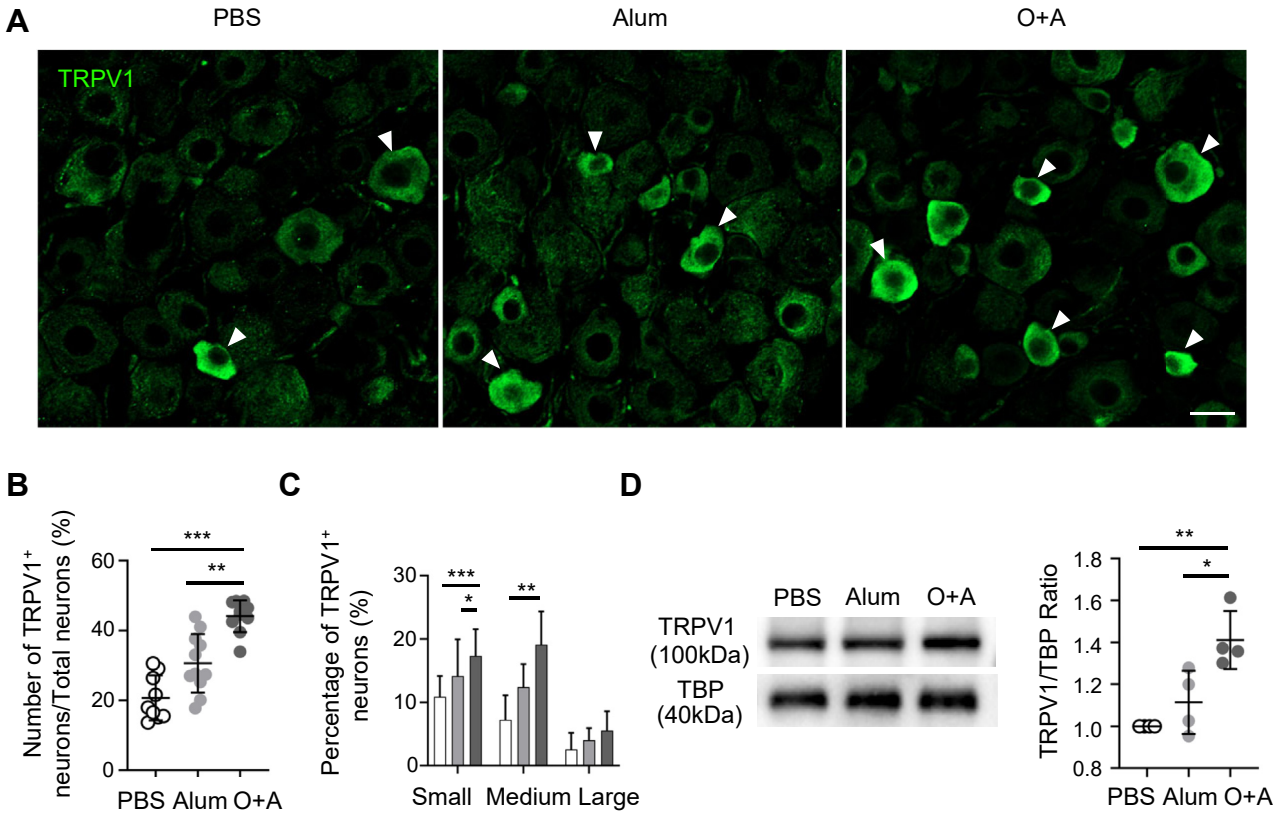

Figure 3.
Enhanced TRPV1 immunoreactivity in the trigeminal ganglion of the atopic asthma mouse model. (A) Representative immunofluorescence images of TRPV1 in the trigeminal ganglion from PBS, Alum, and O+A groups. Arrowheads indicate TRPV1-positive neuronal cell bodies. Airyscan superresolution images. Scale bar = 20 μm. (B) Mean percentage of TRPV1-positive neuronal cell bodies in trigeminal ganglia from PBS, Alum, and O+A groups. n = 3 for each group. (C) Ratios of TRPV1-positive small- (≤300 μm^2), medium- (300-600 μm^2), and large-sized (≥ 600 μm^2) neurons to total neuronal cell bodies in trigeminal ganglia from PBS, Alum, and O+A groups. n = 3 for each group. (D) Immunoblot analysis of TRPV1 in trigeminal ganglia from PBS, Alum, and O+A groups. n = 4 for each group. *P < .05; **P < .01; ***P < .001. Alum, aluminum hydroxide hydrate gel suspension; PBS, phosphate-buffered saline; TRPV1, transient receptor potential channel vanilloid 1.

Gene Expression Microarray Analysis

Total RNA was isolated from trigeminal ganglia with TRIzol reagent (Invitrogen). RNA was purified and analyzed as described previously.[29] Briefly, 50 ng of total RNA was labeled with Cyanine 3. Hybridization was performed on a SurePrint G3 8 × 60K Mouse Gene Expression Arrays (Agilent Technologies). Samples were scanned using an Agilent scanner, and microarray data analysis was performed using Agilent Feature Extraction Software. Raw signal intensities and flags for each probe were calculated from hybridization intensities (gProcessedSignal), while spot information was calculated according to the procedures recommended by Agilent Technologies (Flag criteria on GeneSpring Software), as described previously.[29] To identify upregulated or downregulated genes, we calculated Z scores and ratios (non−log-scaled fold-change) from the normalized signal intensities of each probe for comparison between the control and experimental samples. The Z score was calculated from the $\log_2$ fold-change (logFC) of probes, indicating the distance from the average logFC (eg, if Z score = 2, then logFC of the current probe was 2 × SD from the average). We then used the following criteria for differentially expressed genes: upregulated genes had a Z score ≥ 2.0 and ratio ≥ 1.5-fold, whereas downregulated genes had a Z score of ≤2.0 and a ratio of ≤ 0.66. Microarray data analysis was supported by Cell Innovator.

Experimental Design and Statistical Analysis

Data are expressed as the mean ± SEM for n (number of mice used). Statistical analyses were performed with GraphPad Prism 9 (GraphPad Software Inc), JMP Pro 15 (SAS Institute Inc), or SPSS (Version 25, IBM). The statistical significance of differences in data was analyzed by t test or one-way analysis of variance with Tukey's post hoc analysis. A P value of < .05 was considered significantly different. Significance was labeled as follows: * P < .05, **P < .01, and ***P < .001.

Results

Mechanical Hypersensitivity of Facial Skin in a Mouse Model of Atopic Asthma

A previous report demonstrated that an OVA-induced mouse model of asthma caused a Th2-directed allergic response in C57BL/6 mice.[20] Thus, we performed lung histology and found more PAS-positive mucus cells in the bronchial epithelia of the O+A group compared to controls (Fig. 1B). We did not observe apparent skin lesions or scratching behavior. We tested mechanical sensitivity by applying calibrated von Frey filaments on the whisker pad skin to explore whether atopic asthma led to the

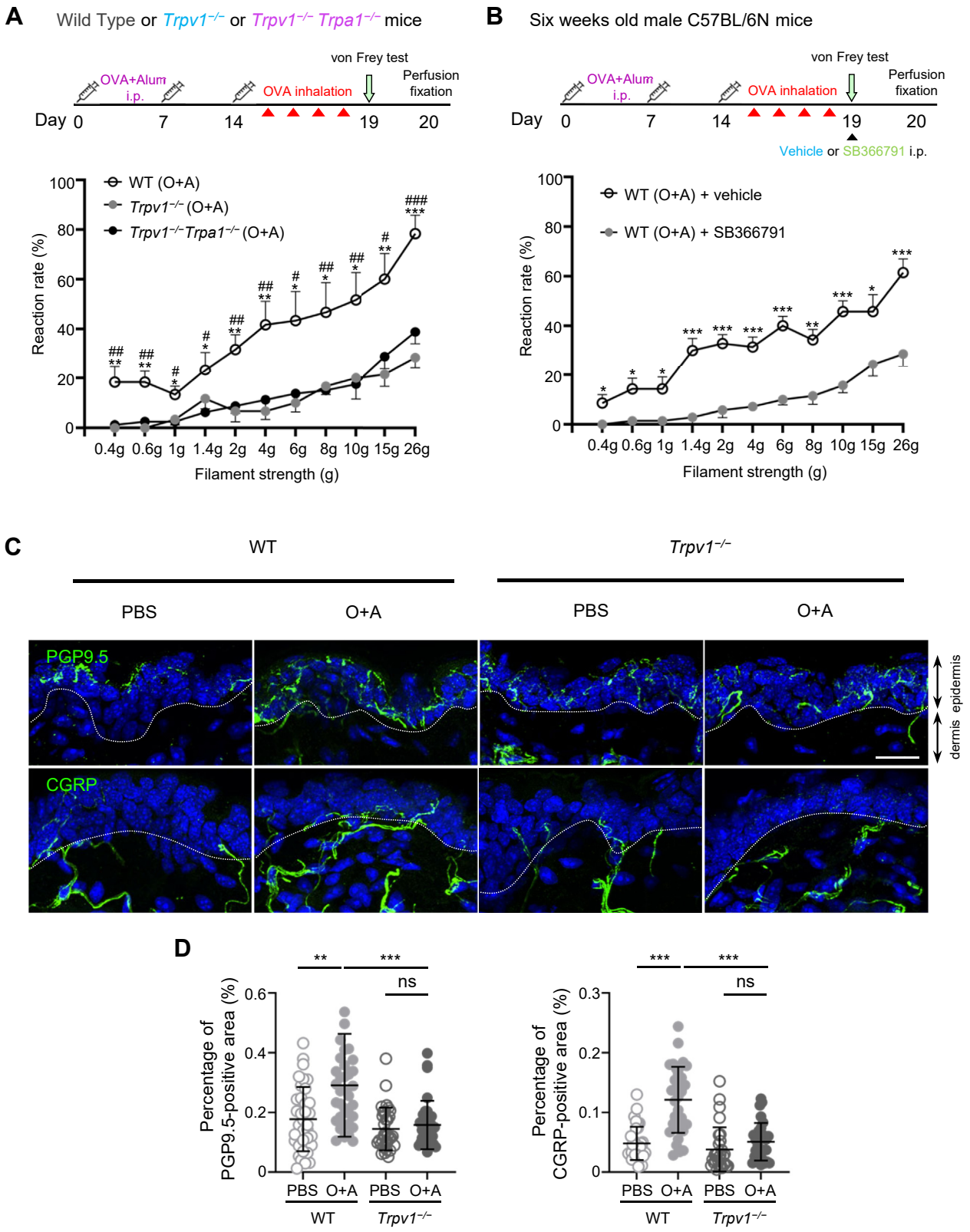

Figure 4.

Attenuated mechanical sensitivity in *Trpv1*-deficient atopic asthma mice. (A) Schematic for atopic asthma model in WT, *Trpv1*$^{-/-}$, and *Trpv1*$^{-/-}$*Trpa1*$^{-/-}$ mice. Reaction rates to different stimulation strengths of von Frey filaments in the atopic asthma model of WT, *Trpv1*$^{-/-}$, and *Trpv1*$^{-/-}$*Trpa1*$^{-/-}$ mice with OVA. Tactile allodynia presented in WT mice by OVA was suppressed in *Trpv1*$^{-/-}$ and *Trpv1*$^{-/-}$*Trpa1*$^{-/-}$ mice. n = 6, 6, and 8, respectively. #*P* < .05; ##*P* < .01; ###*P* < .001. **P* < .05; ***P* < .01; ****P* < .001. #: WT (O+A) vs *Trpv1*$^{-/-}$ (O+A). *: WT (O+A) vs *Trpv1*$^{-/-}$*Trpa1*$^{-/-}$ (O+A). (B) The TRPV1 antagonist SB366791 or vehicle was administered to the facial skin of the mouse model before the von Frey test. Lower reaction rates of O+A mice treated with the TRPV1 antagonist were observed compared with vehicle administration. n = 7 for each group. (C) Representative immunofluorescent images of PGP9.5 and CGRP in facial skin from O+A and PBS groups of WT and *Trpv1*$^{-/-}$ mice. The O+A group exhibited a rich nerve distribution with high

sensitivity of facial skin. The reaction rate to von Frey filaments was significantly higher in the O+A group compared with controls for all stimuli strength except 26 g (Fig. 1C), suggesting that mechanical hypersensitivity of facial skin was evoked in the mouse model with atopic asthma. To investigate the effect of systemic allergies on skin innervation, we examined the distribution of the pan-neuronal marker PGP9.5 to determine whether facial skin hypersensitivity depended on peripheral changes in nerve fibers. We observed abundant PGP9.5-immunoreactive nerve bundles in the dermis and fine fibers that penetrated the epithelia in O+A mice compared to controls (Fig. 1D). Furthermore, we observed increased numbers of TRPV1-immunoreactive nerve fibers with epithelial TRPV1 immunoreactivity in the facial skin of the atopic asthma mouse model compared to the control groups (Fig. 1D). To confirm the TRPV1-immunoreactive fibers in neurons, we coimmunolabeled TRPV1-immunoreactive fibers with PGP9.5. In the facial skin of wild-type (WT) mice, we found that TRPV1-immunoreactive fibers colocalized with PGP9.5, suggesting that TRPV1 localized to the neurons. Under superresolution imaging with an XY-plane resolution of 140 nm, intraepithelial TRPV1 fibers were clearly colocalized with PGP9.5. Epithelial and nervous TRPV1 immunoreactivity were not observed in the skin from *Trpv1*$^{-/-}$ mice (Fig. 1E). These results confirmed the specificity of our TRPV1 antibody against TRPV1. Immunoblotting confirmed elevated levels of TRPV1 expression (100 kDa) in the skin from the O+A group compared to controls (Fig. 1F), suggesting increased epithelial expression of TRPV1 in the mouse model.

Glial Activation in the Trigeminal Ganglion in the Mouse Model of Atopic Asthma

To explore the contribution of peripheral neurons to facial hypersensitivity in the mouse model, we first explored glial activation in the trigeminal ganglion. Immunohistochemistry revealed higher numbers of cells positive for the macrophages/microglia marker Iba-1 in the region of neuronal cell bodies in the O+A group compared with controls (Fig. 2A, B). Iba-1−labeled cells were located along blood vessels or juxtaposed to neuronal cell bodies and not found in the nerve fiber region. Changes in the shape of microglia or macrophages from ramified to amoeboid are a reported indicator of microglia activation.[30] In our study, the mean area, perimeter, and Feret's diameter of Iba-1 cells were significantly larger in the O+A group compared to controls. Moreover, Iba-1-immunoreactive cells showed lower circularity and a higher aspect ratio in the O+A group compared to controls. Furthermore, there were significant differences between the PBS and Alum groups in microglial density, perimeter, circularity, and Feret diameter (Fig. 2C), indicating longer and thicker cytoplasmic processes and multiple ramifications of microglia in the O+A group. These results suggest that under the conditions of asthma, microglia/macrophage activation with characteristic morphologic changes occurred in the trigeminal ganglion. Recently, an active role of satellite glial cells in the process of chronic pain has been reported in DRG and the trigeminal ganglion.[31] To address the contribution of satellite glial activation to hypersensitivity, we examined phosphorylation of extracellular regulated kinase (pERK), an essential signaling pathway involved in various cellular processes such as cell proliferation and differentiation that is also used as a glial activation marker.[32] In the trigeminal ganglion, neuronal cell bodies were wrapped by pERK-immunoreactive satellite glial cells, while Iba-1−immunoreactive cells were located among the intercellular space of satellite glial cells. Higher pERK immunoreactivity was observed around larger neuronal cell bodies in the O+A group compared to controls (Fig. 2A, D). Immunoblotting confirmed enhanced pERK expression in the trigeminal ganglia of the O+A group compared to controls (Fig. 2E). Thus, atopic asthma led to the activation of microglia/macrophages and satellite glial cells in the trigeminal ganglion.

Enhanced TRPV1 Immunoreactivity in the Trigeminal Ganglia of the Mouse Model of Atopic Asthma

Accumulating reports indicate that TRPV1 plays critical roles in nociception, pain, and itch,[33] and is dynamically regulated during allergic inflammation with tissue insult. We immunohistochemically examined TRPV1 in the trigeminal ganglion. Primary sensory neuronal cell bodies were classified as small ($\leq$300 μm^2), medium (300-600 μm^2), or large ($\geq$ 600 μm^2) according to their soma areas.[34] In controls, TRPV1 immunoreactivity was observed in small- to medium-sized neurons (Fig. 3A). In the O+A group, more small- to medium-sized TRPV1 positive neurons were observed, and the number of TRPV1-positive neurons were higher than that in controls (Fig. 3B, C). The numbers of large-sized TRPV1-positive neurons tended to increase in the O+A group compared to controls (Fig. 3C). Immunoblotting confirmed elevated TRPV1 expression in trigeminal ganglia of the O+A group compared to controls (Fig. 4D). Collectively, these results suggest that TRPV1 expression in neurons is associated with facial mechanical hypersensitivity in the mouse model.

Trpv1 Deficiency Attenuated Mechanical Sensitivity Induced by Atopic Asthma

Next, we investigated whether the effect of TRPV1 on facial sensitization was maintained in *Trpv1*-deficient (*Trpv1*$^{-/-}$) mice. After OVA sensitization, *Trpv1*$^{-/-}$ mice showed lower reaction rates in facial von Frey tests than WT mice. We also found that the reaction rate of von Frey filaments in *Trpv1*$^{-/-}$*Trpa1*$^{-/-}$ mice was similar to that in *Trpv1*$^{-/-}$ mice (Fig. 4A). Next, to explore whether a topical TRPV1 antagonist suppressed mechanical hypersensitivity, we subcutaneously injected the selective TRPV1 antagonist SB366791 into the facial skin of OVA-treated mice. Tactile behavior was efficiently inhibited in the SB366791 injected group for all ranges of von Frey fiber stimulus strength in the mouse model (Fig. 4B). To evaluate the effect of TRPV1 on skin innervatio, we immunohistochemically observed PGP9.5-immunoreactive nerves. We did not observe significant differences between PBS- and OVA-treated *Trpv1*$^{-/-}$ mice (Fig. 4C, D). We also explored the distribution of CGRP, a neuropeptide mediator of neurogenic vasodilatation related to mechanical allodynia[35]. OVA-treated WT mice showed intense CGRP-immunoreactive nerve fibers in their facial skin, whereas OVA-treated *Trpv1*$^{-/-}$ mice showed fewer CGRP-labeled nerve fibers than OVA-treated WT mice (Fig. 4C, D). These results suggest that TRPV1 contributes to tactile orofacial allodynia in the mouse model.

PGP9.5 and CGRP expression compared with the PBS group, while distributions were similar between O+A and PBS groups of *Trpv1*$^{-/-}$ mice. Images acquired by BC43. Scale bar = 10 μm. (D) Quantification of PGP9.5- and CGRP-positive areas of facial skin from O+A and PBS groups of WT and *Trpv1*$^{-/-}$ mice, respectively. n = 3 for each group. *P < .05; **P < .01; ***P < .001. CGRP, calcitonin gene-related peptide; OVA, ovalbumin; PBS, phosphate-buffered saline; WT, wild type;

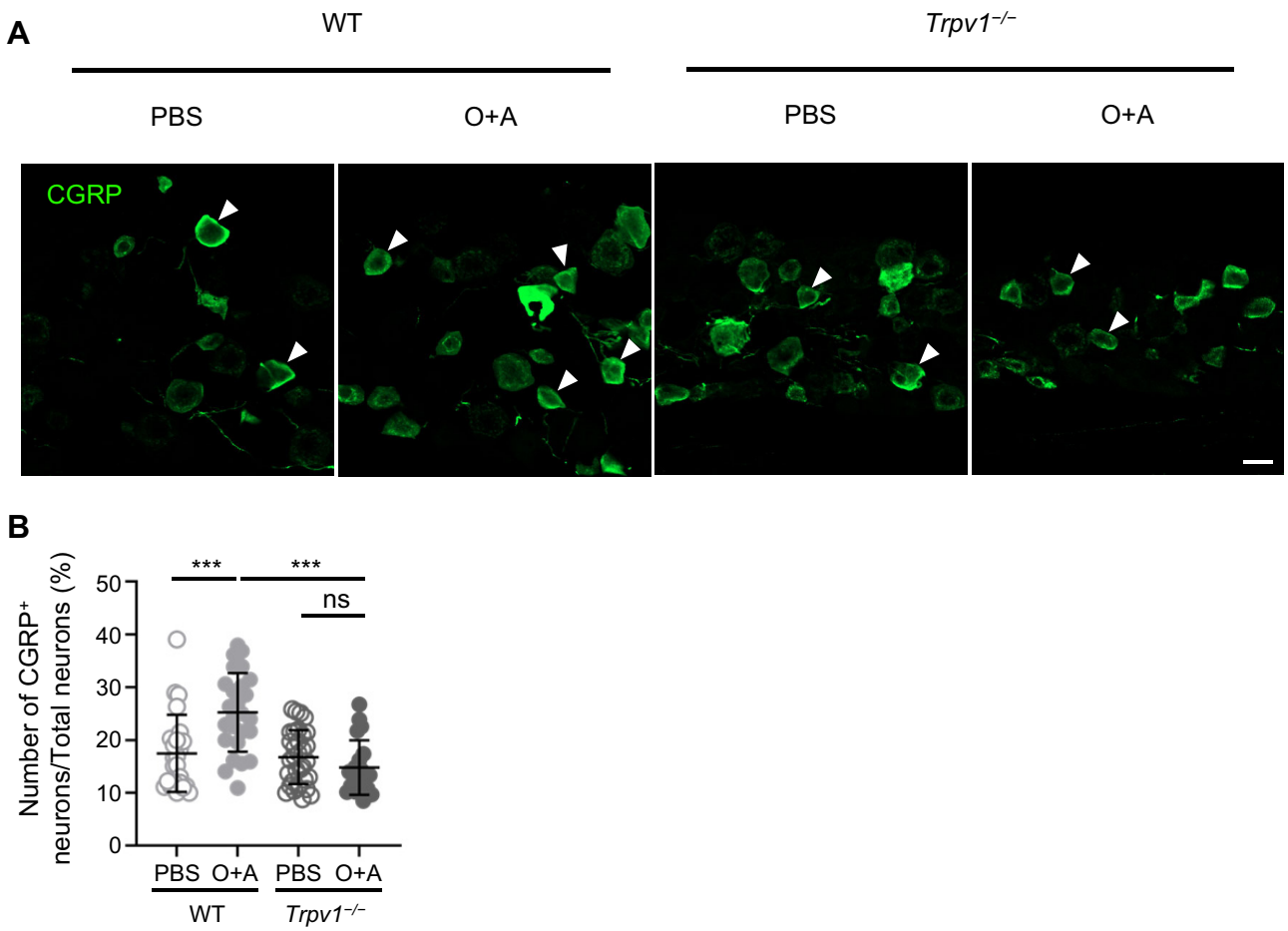

Figure 5.
Induction of asthma did not increase the number of trigeminal CGRP neurons in *Trpv1*-deficient mice. (A) Representative immunofluorescent images of CGRP in trigeminal ganglia from PBS and O+A groups of WT and *Trpv1*$^{-/-}$ mice. Arrowheads indicate CGRP-positive neurons. Airyscan superresolution images. Scale bar = 20 μm. (B) Mean percentage of CGRP-positive neurons in trigeminal ganglia from PBS and O+A groups of WT and *Trpv1*$^{-/-}$ mice. n = 3 for each group. ***$P < .001$. CGRP, calcitonin gene-related peptide; PBS, phosphate-buffered saline; WT, wild type.

Trpv1 Deficiency Suppressed Asthma-Induced Increases of CGRP Neurons in the Trigeminal Ganglion

Next, we explored the impact of TRPV1 on atopic asthma-induced neuronal activation by immunohistochemically observing CGRP expression. There were larger numbers of CGRP-positive neuronal cell bodies in the trigeminal ganglia of OVA-treated WT mice than in PBS-treated WT mice. However, compared with *Trpv1*$^{-/-}$ mice, OVA treatment did not increase the number of CGRP-immunoreactive cell bodies in the trigeminal ganglion (Fig. 5A, B). These results suggest that TRPV1 upregulation led to an increased number of CGRP-immunoreactive neurons in the trigeminal ganglia of the mouse model.

Varied Actin Filament Distribution in the Trigeminal Ganglion in the Mouse Model of Atopic Asthma

To explore the molecular mechanisms underlying mechanical sensitivity, we performed an RNA array assay of trigeminal ganglia among the 3 experimental groups. Among genes with apparent differences between the groups, we observed remarkable changes in actin, one of the most abundant and essential cytoskeletal proteins for cell behavior and tissue integrity. The functions of actin in nervous tissues have been well-studied in the central nervous system, such as pathologic synaptic plasticity in dendritic spines. However, few studies have evaluated the relationship between actin and primary sensory ganglia. We found that *Acta1* and *Acta2* expressions were significantly downregulated in the O+A group compared to the PBS group (Z score = −2.44 and −3.43, respectively; fold increases of 0.62 and 0.37, respectively).

To explore the effect of actin filaments, we utilized fluorescent phalloidin to reveal the distribution of filamentous actin in the trigeminal ganglion. In WT mice, actin filaments (F-actin) were intensely distributed in the region of neuronal cell bodies, while distinct small spots of actin filaments were observed in the region of nerve fibers (Fig. 6A). Intense bundles of F-actin wrapped around almost all neuronal cell bodies. The thick bundles of F-actin enveloped larger neuronal cell bodies, whereas the thin bundles wrapped around smaller neuronal cell bodies. Short and thin F-actin was observed in the cytoplasm of neuronal cell bodies (Fig. 6A). F-actin staining also delineated blood vessels (Fig. 6A). To define whether actin filaments were inside or outside of the neuronal cell bodies, we employed superresolution laser-scanning microcopy. The results revealed intense F-actin bundles that colocalized with the satellite cell marker S100β and pERK (Fig. 6B). The line profile of neuronal cell-cell boundaries showed clear

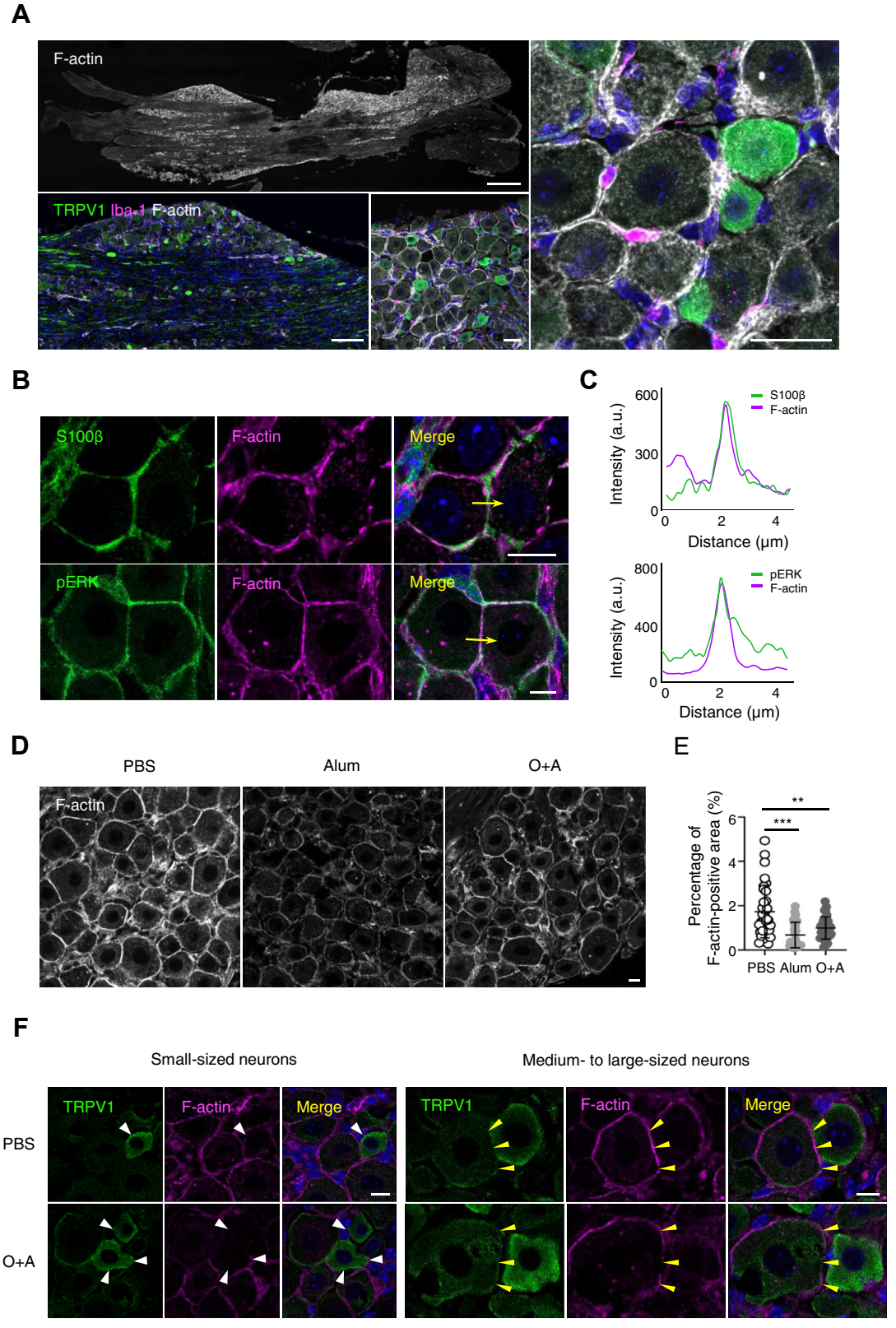

Figure 6.
Changes in actin fiber distribution in the trigeminal ganglia of the mouse model of atopic asthma. (A) Representative images of staining for TRPV1 (green) and Iba-1 (magenta), and F-actin (white) in trigeminal ganglia of WT mice. Images acquired by BC43. A horizontal section of the dorsal part of the trigeminal ganglion showing F-actin located in the region containing neuronal cell bodies. The F-actin network wrapped neuronal cell bodies. Distinct Iba-1 immunoreactivity in the intercellular space of neuronal cell bodies. Thicknesses of actin fibers were larger around larger neuronal cell bodies. Scale bars = 300 μm, 100 μm, and 20 μm, respectively. (B) Airyscan images of trigeminal ganglia double-stained for S100β (green) and F-actin (magenta), pERK (green), and F-actin (magenta), respectively. Scale bar = 10 μm. (C) The line profile of F-actin and S100β

colocalization of F-actin and S100β or pERK (Fig. 6C), suggesting that thick conspicuous actin filaments were outside of neuronal cell bodies and located in satellite glial cells. We found that some F-actin was localized in Iba-1−immunoreactive cells. Satellite glia with actin filaments closely wrapped around the neuronal cell bodies and larger neuronal cell bodies had thicker actin filaments than the smaller neuronal cell bodies, suggesting that the actin filament covering might affect the sensory properties of the primary neurons.

To examine whether the asthmatic condition affected F-actin expression levels, we compared the 3 groups. F-actin−stained areas were significantly decreased in the O+A group compared to controls (Fig. 6D, E). The F-actin wrapped neuronal cell bodies in the WT group had a somewhat straight line, whereas those in the O+A group had a delicate, wavy, and faint line (Fig. 6F). Larger neuronal cell bodies had a conspicuous envelope of F-actin without TRPV1-immunoreactivity, whereas smaller neuronal cell bodies with TRPV1 had thin F-actin in the PBS and O+A groups. Furthermore, in the O+A group, TRPV1-positive neuronal cell bodies had less actin filaments than those in the PBS group (Fig. 6F). The surface outline of the neuronal cell bodies with TRPV1 in the O+A group had a thin, rough, and wavy line compared to the PBS group (Fig. 6F). This suggested that smaller neuronal cell bodies with TRPV1, wrapped by a thin actin covering, might be susceptible to the structural derangements of the cell shape.

Trpv1 Deficiency Suppressed Glial Activation in the Trigeminal Ganglion

To explore the effect of TRPV1 on glial activation, we immunohistochemically compared the distributions of Iba-1, F-actin, and pERK (Fig. 7A). The number of Iba-1−immunoreactive cells in the trigeminal ganglion was higher in OVA-treated WT mice than in PBS-treated WT mice, but this increase was not observed in OVA-treated *Trpv1*$^{-/-}$ mice. In addition, increased areas of pERK immunoreactivity in OVA-treated WT mice were not observed in OVA-treated *Trpv1*$^{-/-}$ mice. The area positive for F-actin was distinctly diminished in OVA-treated WT mice compared to PBS-treated WT mice but similar between PBS- and O+A−treated *Trpv1*$^{-/-}$ mice. The F-actin cellular outline was faint and wavy in O+A−treated WT mice compared to the PBS group, but that was not observed between PBS- and O+A−treated *Trpv1*$^{-/-}$ mice. Quantitative analyses confirmed these subjective observations (Fig. 7B, C). Collectively, these results suggest that TRPV1 plays an upstream role in microglia/macrophage activation and structural disorganization of satellite glial F-actin.

Discussion

The sense of touch exhibits a wide range of sensitivity to detect the physical properties of the external environment. Patients with atopic allergic diseases manifest sensitive skin. Even without skin lesions, these individuals detect a single hair on the face with uncomfortable perception, which normally should not raise such unpleasantness. Because facial hypersensitivity causes more unpleasantness than other regions of the body, we attempted to elucidate the mechanisms underlying the sensitive skin in the orofacial region with atopic diseases by utilizing a mouse atopic asthma model with OVA sensitization. We used the von Frey test to observe the mechanical hypersensitivity of the facial skin of the mouse model without apparent skin lesions or scratching behaviors. An increasing number of patients with sensitive skin also have a history of allergic disease[7], which begins in infancy with atopic dermatitis and food allergy and subsequently develops into allergic rhinitis or asthma. We utilized a mouse model of atopic asthma that represents a typical allergic inflammatory disease of the airways, which frequently accompanies other allergic diseases such as atopic dermatitis or rhinitis. We suggest that OVA-sensitized mice could be one of the mouse models for understanding the pathology of patients affected by subjective facial skin unpleasantness.

Orofacial skin has rich innervation to perceive changes in the environment. Compared with controls, the mouse model showed elevated mechanical reactions in response to von Frey fibers. This mechanical hyperreactivity is similar to our previous report describing the plantar hind paw[29], suggesting that atopic asthma induced by OVA sensitization may lead to the systemic mechanical hypersensitivity of the skin. Labeling cells with the pan-neuronal marker PGP9.5 showed us more intense innervation, especially of intraepithelial nerves in the O+A group, than in controls (Fig. 8). The mouse model showed richer TRPV1-immunoreactive nerve fibers in the facial skin and increased TRPV1 expression in epithelial keratinocytes. TRPV1 plays a significant role in the pathophysiology of asthma and chronic cough[36]. Moreover, TRPV1 was reportedly overexpressed in the bronchial epithelia of patients with severe asthma compared to patients with mild asthma and healthy subjects[37]. The increased distribution of TRPV1-immunoreactive skin nerve fibers and expression of TRPV1 in skin keratinocytes may contribute to the mechanical hypersensitivity of facial skin. This idea is supported by the results demonstrating that topical application of the TRPV1 antagonist SB366791 could suppress mechanical hypersensitivity. Accumulating findings suggest that critical Th2-related cytokines, such as interleukin (IL)-13[38] or IL-31[39], potentiate TRPV1 transcription and channel activity. The systemic Th2 response induced by OVA sensitization increased facial skin nerve supply and induced both neuronal and epidermal TRPV1 expression, leading to hypersensitivity.

In the trigeminal ganglia of the mouse model, we observed significantly larger numbers of TRPV1-immunoreactive cell bodies in small- to medium-sized neurons compared to controls, and the same tendency was observed for large-sized neurons (Fig. 8). Enhanced TRPV1 expression was confirmed by immunoblotting crude extracts of trigeminal ganglia. The size of cell bodies reflects functional differences; specifically, small- to medium-sized neurons transduce nociceptive information, while larger neurons transduce innocuous mechanical forces initiated by proprioceptors and cutaneous touch receptors[40]. OVA sensitization−induced neuronal plasticity and elevated TRPV1 expression in larger neuronal cell bodies compared with controls, potentially leading to mechanical allodynia and hyperalgesia. Furthermore, mechanical hypersensitivity in the atopic asthma model was significantly reduced in

colocalization or pERK is indicated by arrows. Clear colocalization is observed in the peak of these 2 immunoreactivity profiles. (D) Representative immunofluorescent images of F-actin in trigeminal ganglia of PBS, Alum, and O+A groups. Images acquired by BC43. Scale bar = 10 μm. (E) Quantification of F-actin−positive area in trigeminal ganglia of PBS, Alum, and O+A groups (n = 3 for each group). (F) Representative immunofluorescent Airyscan superresolution images of TRPV1 and F-actin in trigeminal ganglia of PBS and O+A groups. Small-sized TRPV1-positive neuronal cell bodies (white arrowheads) contained less F-actin, whereas medium- or large-sized neurons (yellow arrowheads) displayed intense F-actin with less TRPV1-immunoreactivity. Scale bar = 10 μm. $^{**}P < .01$; $^{***}P < .001$. Iba-1, ionized Ca^{2+} binding adapter molecule 1; PBS, phosphate-buffered saline; pERK, phospho-p44/42 MAPK; TRPV1, transient receptor potential channel vanilloid 1; WT, wild type.

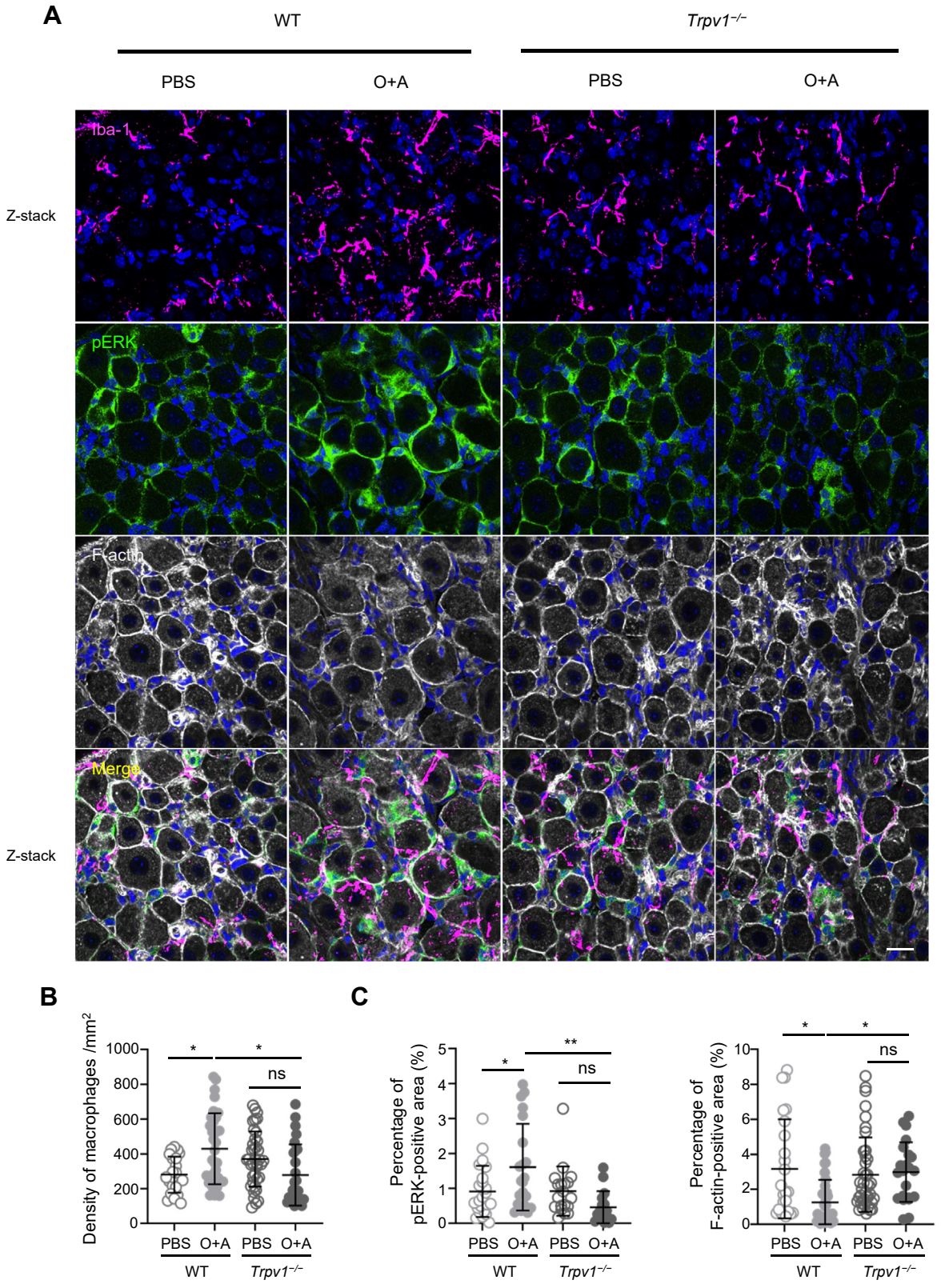

Figure 7.

Glial activation in the trigeminal ganglion was reduced in *Trpv1*-deficient mice. (A) Representative immunofluorescent images of pERK (green), Iba-1 (magenta), and F-actin (white) in trigeminal ganglia from O+A and PBS groups of WT and *Trpv1*$^{-/-}$ mice. Images were acquired by BC43. OVA sensitization–induced phosphorylation of ERK and increased numbers of Iba-1-immunoreactive cells in WT mice but not in *Trpv1*$^{-/-}$ mice. OVA sensitization–induced suppression of F-actin was not observed in *Trpv1*$^{-/-}$ mice. Top and merged images showing Iba-1 processed with an orthogonal projection of 7 μm. pERK- and F-actin images showing single optical slice. Scale bar = 20 μm. (B) Quantitative analysis of microglial cell density in trigeminal ganglia from O+A and PBS groups of WT and *Trpv1*$^{-/-}$ mice. (C) Quantification of pERK- and F-actin–positive areas in trigeminal ganglia from O+A and PBS groups of WT and *Trpv1*$^{-/-}$ mice. n = 3 for each group. *P < .05; **P < .01. Iba-1, ionized Ca^{2+} binding adapter molecule 1; OVA, ovalbumin; PBS, phosphate-buffered saline; pERK, phospho-p44/42 MAPK; TRPV1, transient receptor potential channel vanilloid 1; WT, wild type.

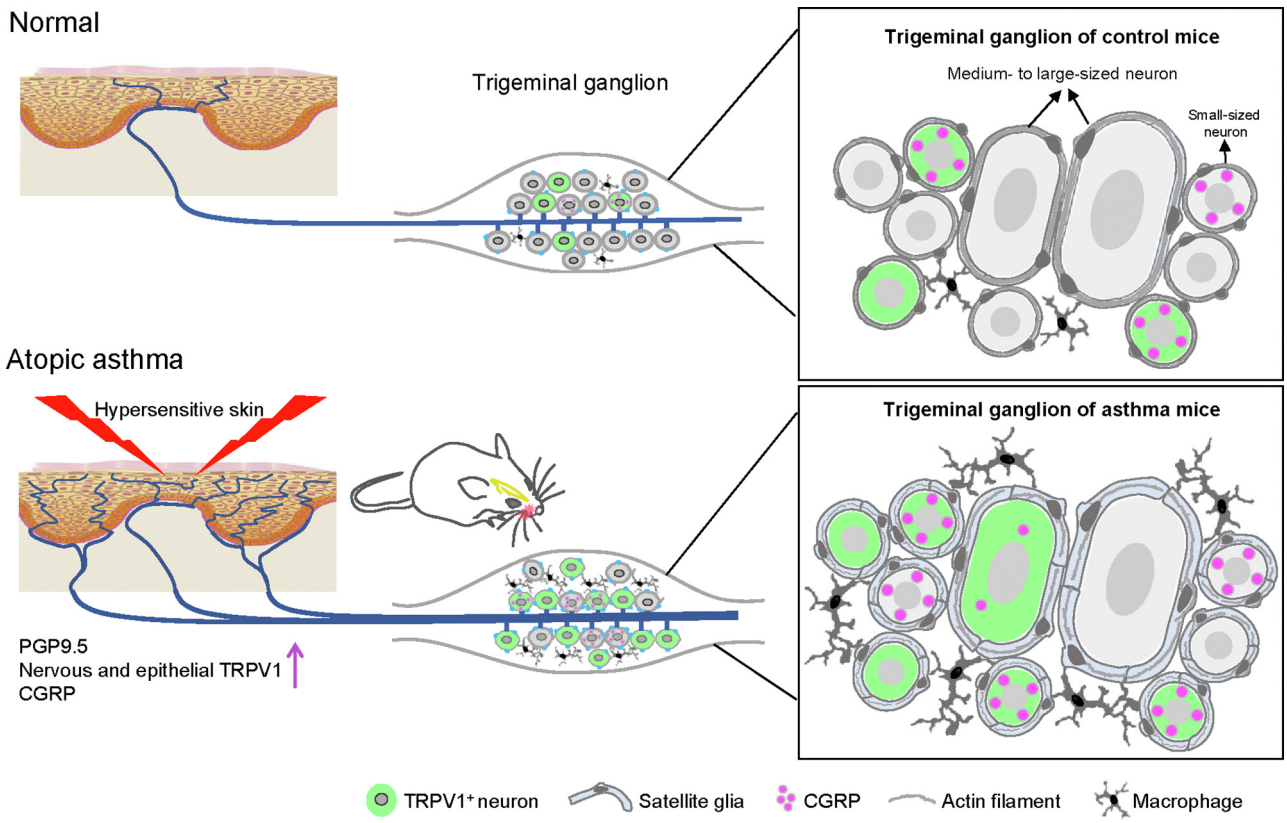

Figure 8.
Schematic representation of differences in skin and trigeminal ganglia between normal and atopic asthma mice. Atopic asthma evoked mechanical hypersensitivity of facial skin with rich PGP9.5, CGRP, and TRPV1 peripheral nerves. In the trigeminal ganglion, neuronal plasticity with enhanced TRPV1 and CGRP expression and activated macrophage/microglia and satellite glia were observed. Neuronal cell bodies were wrapped by bundles of actin filaments; however, the asthmatic condition weakened this filamentous actin network. Facial hypersensitivity is potentially mediated by TRPV1-dependent glial and neuronal plasticity. CGRP, calcitonin gene-related peptide; TRPV1, transient receptor potential channel vanilloid 1.

Trpv1$^{-/-}$ mice compared with that in WT mice, suggesting that TRPV1 is one of the main modulators of this behavior under the atopic asthma condition. Previous studies in mice demonstrated that both TRPV1- and TRPA1-expressing DRG neurons are important contributors to scratching[41] and pain[33] behavior. We expected that OVA-treated double-knockout (*Trpv1*$^{-/-}$*Trpa1*$^{-/-}$) mice would show reduced responses to mechanical stimuli compared to OVA-treated *Trpv1*$^{-/-}$ mice; however, their reaction rates were similar. Recently, mechanosensitive ion channels Piezo1 and Piezo2, which are expressed in the trigeminal ganglion[42], have been associated with tactile pain in mice and humans.[43,44] In addition to TRPV1, TRPA1 and Piezo channels could contribute to atopic facial mechanical hypersensitivity. Further studies are needed to characterize the properties of trigeminal ganglion neurons in facial sensitization because the trigeminal sensory ganglion has variable distinct characteristics from the spinal sensory system under physiological or pathologic conditions.[45]

Microglia/macrophages and satellite glial cells participate in the development and maintenance of chronic pain.[46] We observed activation (increased Iba-1 and pERK immunoreactivity) of microglia/macrophages and satellite glial cells in the trigeminal ganglia of the mouse model. This result of systemic OVA sensitization—induced glial activation is consistent with a previous report on the spinal cord.[29] The functional state of microglia/macrophages can be characterized by cellular morphologic changes.[47] Microglia/macrophages in the trigeminal ganglion of the mouse model were larger and longer, with thicker and flattened cytoplasmic processes than in the PBS group. These morphologic characteristics are not consistent with previous reports in the spinal cord of an atopic model[29] or brain.[48] Iba-1—immunoreactive cells were located in the intercellular space adjacent to the neuronal cell bodies. In addition, these cells were juxtaposed to blood vessels, suggesting that some activated microglia/macrophages may have been recruited from circulating blood cells. Activation of microglia/macrophages and satellite glial cells was not observed in OVA-treated *Trpv1*$^{-/-}$ mice. These results suggest that glial activation was downstream of TRPV1, which may affect both neuronal and glial plasticity in the trigeminal ganglion.

Recently, an emerging role of neuron-satellite glia interactions was implicated in chronic pain.[31] We observed enhanced pERK; otherwise, less F-actin was observed in satellite glial cells of the mouse model compared to controls. F-actin bundles were conspicuous around large neuronal somata, whereas thin fibers were observed around small neurons. Neuronal cell bodies had intracellular actin filaments but not cortical actin, suggesting that satellite glial actin bundles provided structural support to neuronal somata. Increasing evidence shows that cortical actin plays a significant role in controlling the cell shape, resisting external mechanical stresses, and exertion of forces on neighboring cells.[49] Neurons and satellite glial cells in the sensory ganglia communicate bidirectionally, reportedly through chemical messengers.[50]

Accordingly, satellite glial cells may play a role in regulating the mechanical properties of neurons. This notion is supported by the morphologic observation of rather faint and weak flaccid edge contours in the neuronal somata of the mouse model. The actin cytoskeleton is integral to peripheral glial migration and neurolemma and mediated by RhoA and Rac1.[51] Satellite glial cells in the DRG reportedly participate in acute nociception induced by capsaicin stimulation.[52] Furthermore, Feldman-Goriachnik et al[50] showed that capsaicin-induced activation of satellite glial cells and neuron-satellite glia coupling is upregulated by systemic inflammation. This study showed that Th2-directed systemic conditions with airway sensitization—evoked facial sensitization might be caused by neuronal-satellite glial interactions, which have similar underlying mechanisms to LPS-induced inflammation in the trigeminal ganglion.[53] Evidence indicates that actin remodeling modifies neuronal properties such as channel activity and synaptic plasticity in the neuronal cell body, dendrites, or spines in the central nervous system.[54,55] However, further molecular and morphologic analyses are needed to explore how direct interactions between satellite glia and neurons affect neuronal or glial plasticity from systemic and peripheral aspects.

TRPV1 appears to play a role in sensitive skin through increased peripheral innervation and glial and neuronal activation in the trigeminal ganglion. The mechanistic pathways of TRPV1 remain unclear because functional TRPV1 is expressed in a variety of cell types, including peripheral sensory neurons and non-neuronal cells such as epithelia, blood vessel walls, and immune cells[56]. The contribution of TRPV1 to the development of asthma was demonstrated by the administration of the TRPV1 antagonist capsazepine or TRPV1 small-interfering RNA, which suppressed peribronchial inflammation and Th2 cytokine release in OVA-treated BALB/c mice[57]. The level of airway inflammation was indistinguishable between OVA-sensitized *Trpv1*$^{-/-}$ mice and WT mice[20]. This suggested that the suppression of neuronal and glial activation in the trigeminal ganglion or in the skin of the OVA-treated *Trpv1*$^{-/-}$ mice in this study might not result from the suppression of Th2 asthmatic responses. Clinical trials of the oral TRPV1 antagonist SB-705498[58] or XEN-D0501[59] administered to patients with refractory chronic cough did not reduce the objective cough frequency. However, a topical TRPV1 inhibitor was recently reported to improve the severity of perioral dermatitis[60]. Based on these findings, topical or systemic administration of a TRPV1 inhibitor might be an attractive approach to suppress facial mechanical hypersensitivity, a common manifestation of allergic individuals, which could improve patients' quality of life.

Acknowledgments

The authors thank Prof. M. Tominaga from the National Institute for Physiological Sciences for generously providing *Trpv1*$^{-/-}$ mice and *Trpv1*$^{-/-}$*Trpa1*$^{-/-}$ mice. The authors thank Prof. Y. Murata, Dr. M. Nishiyama, and Dr. Y. Honda for technical assistance. The authors thank Prof. M. Shinoda for his expert advice on the von Frey test. The authors also thank Prof. T. Kiyoshima for their experimental advice. The authors are grateful to the Division of Biological Resources and Development, Analytical Research Center for Experimental Sciences of Saga University, for animal care and the Division of Instrumental Analysis, Analytical Research Center for Experimental Sciences of Saga University, for technical assistance. The authors thank J. Ludovic Croxford from Edanz (https://jp.edanz.com/ac) for editing a draft of this manuscript. This study is based on the doctoral thesis of A.C., submitted to the graduate school of Kyushu University as a fulfillment of the requirements for the PhD degree.

Author Contributions

M.A.K. conceived, designed, and supervised the study. A.-L.C., W.-Q.G., R.U.Y., R.A., T.S., and M.A.K. performed the experiments. A.-L.C., W.-Q.G., and T.S. performed acquisition and analysis of data, and statistical analysis. Y.O. generated the TRPV1 antibody. A.-L.C. and M.A.K. wrote the manuscript.

All authors read and approved the final paper.

Data Availability

The data sets used and/or analyzed during the current study are available from the corresponding author upon reasonable request.

Funding

This study was supported by operational funds from Saga University.

Declaration of Competing Interest

The authors declare no competing interests.

References

1. Basbaum AI, Bautista DM, Scherrer G, Julius D. Cellular and molecular mechanisms of pain. *Cell*. 2009;139(2):267–284. https://doi.org/10.1016/j.cell.2009.09.028
2. Metze D. Neuroanatomy of the skin. In: Granstein RD, Luger TA, eds. *Neuroimmunology of the Skin*. 1st ed. Springer; 2009:3–12.
3. Berardesca E, Farage M, Maibach H. Sensitive skin: an overview. *Int J Cosmet Sci*. 2013;35(1):2–8. https://doi.org/10.1111/j.1468-2494.2012.00754.x
4. Misery L, Ständer S, Szepietowski JC, et al. Definition of sensitive skin: an expert position paper from the special interest group on sensitive skin of the international forum for the study of itch. *Acta Derm Venereol*. 2017;97(1):4–6. https://doi.org/10.2340/00015555-2397
5. Farage MA. The prevalence of sensitive skin. *Front Med (Lausanne)*. 2019;6:98. https://doi.org/10.3389/fmed.2019.00098
6. Eder W, Ege MJ, von Mutius E. The asthma epidemic. *N Engl J Med*. 2006;355(21):2226–2235. https://doi.org/10.1056/NEJMra054308
7. Willis CM, Shaw S, De Lacharrière O, et al. Sensitive skin: an epidemiological study. *Br J Dermatol*. 2001;145(2):258–263. https://doi.org/10.1046/j.1365-2133.2001.04343.x
8. Kira J, Yamasaki K, Kawano Y, Kobayashi T. Acute myelitis associated with hyperIgEemia and atopic dermatitis. *J Neurol Sci*. 1997;148(2):199–203. https://doi.org/10.1016/s0022-510x(97)05369-0
9. Isobe N, Kira J, Kawamura N, Ishizu T, Arimura K, Kawano Y. Neural damage associated with atopic diathesis: a nationwide survey in Japan. *Neurology*. 2009;73(10):790–797. https://doi.org/10.1212/WNL.0b013e3181b6bb6b
10. Van Gerven L, Alpizar YA, Wouters MM, et al. Capsaicin treatment reduces nasal hyperreactivity and transient receptor potential cation channel subfamily V, receptor 1 (TRPV1) overexpression in patients with idiopathic rhinitis. *J Allergy Clin Immunol*. 2014;133(5):1332–1339.e3. https://doi.org/10.1016/j.jaci.2013.08.026
11. Acosta CM, Luna C, Quirce S, Belmonte C, Gallar J. Changes in sensory activity of ocular surface sensory nerves during allergic keratoconjunctivitis. *Pain*. 2013;154(11):2353–2362. https://doi.org/10.1016/j.pain.2013.07.012
12. Balestrini A, Joseph V, Dourado M, et al. A TRPA1 inhibitor suppresses neurogenic inflammation and airway contraction for asthma treatment. *J Exp Med*. 2021;218(4):e20201637. https://doi.org/10.1084/jem.20201637
13. Meng J, Li Y, Fischer MJM, Steinhoff M, Chen W, Wang J. Th2 modulation of transient receptor potential channels: an unmet therapeutic intervention for atopic dermatitis. *Front Immunol*. 2021;12, 696784. https://doi.org/10.3389/fimmu.2021.696784

14. Nam JH, Kim WK. The role of TRP channels in allergic inflammation and its clinical relevance. *Curr Med Chem*. 2020;27(9):1446–1468. https://doi.org/10.2174/0929867326666181126113015
15. Bereiter DA, Hargreaves KM, Hu JW. Trigeminal mechanisms of nociception: peripheral and brainstem organization. In: Masland RH, Albright TD, Albright TD, et al., eds. *The Senses: A Comprehensive Reference*. Academic Press; 2008:435–460. https://doi.org/10.1016/B978-012370880-9.00174-2
16. Urata K, Shinoda M, Honda K, et al. Involvement of TRPV1 and TRPA1 in incisional intraoral and extraoral pain. *J Dent Res*. 2015;94(3):446–454. https://doi.org/10.1177/0022034514565645
17. Honda K, Shinoda M, Furukawa A, Kita K, Noma N, Iwata K. TRPA1 contributes to capsaicin-induced facial cold hyperalgesia in rats. *Eur J Oral Sci*. 2014;122(6):391–396. https://doi.org/10.1111/eos.12157
18. Caterina MJ, Leffler A, Malmberg AB, et al. Impaired nociception and pain sensation in mice lacking the capsaicin receptor. *Science*. 2000;288(5464):306–313. https://doi.org/10.1126/science.288.5464.306
19. Bautista DM, Sigal YM, Milstein AD, et al. Pungent agents from Szechuan peppers excite sensory neurons by inhibiting two-pore potassium channels. *Nat Neurosci*. 2008;11(7):772–779. https://doi.org/10.1038/nn.2143
20. Caceres AI, Brackmann M, Elia MD, et al. A sensory neuronal ion channel essential for airway inflammation and hyperreactivity in asthma. *Proc Natl Acad Sci U S A*. 2009;106(22):9099–9104. https://doi.org/10.1073/pnas.0900591106
21. Kamp EH, Jones RCW, Tillman SR, Gebhart GF. Quantitative assessment and characterization of visceral nociception and hyperalgesia in mice. *Am J Physiol Gastrointest Liver Physiol*. 2003;284(3):G434–G444. https://doi.org/10.1152/ajpgi.00324.2002
22. Chaplan SR, Bach FW, Pogrel JW, Chung JM, Yaksh TL. Quantitative assessment of tactile allodynia in the rat paw. *J Neurosci Methods*. 1994;53(1):55–63. https://doi.org/10.1016/0165-0270(94)90144-9
23. Labuz D, Spahn V, Celik MÖ, Machelska H. Opioids and TRPV1 in the peripheral control of neuropathic pain – defining a target site in the injured nerve. *Neuropharmacology*. 2016;101:330–340. https://doi.org/10.1016/j.neuropharm.2015.10.003
24. Yoshimoto RU, Aijima R, Ohyama Y, et al. Impaired junctions and invaded macrophages in oral epithelia with oral pain. *J Histochem Cytochem*. 2019;67(4):245–256. https://doi.org/10.1369/0022155418812405
25. Takayama Y, Uta D, Furue H, Tominaga M. Pain-enhancing mechanism through interaction between TRPV1 and anoctamin 1 in sensory neurons. *Proc Natl Acad Sci U S A*. 2015;112(16):5213–5218. https://doi.org/10.1073/pnas.1421507112
26. A practical guide of deconvolution application. Zeiss. Accessed March 22, 2023. https://asset-downloads.zeiss.com/catalogs/download/mic/86baa56d-3854-4eda-a342-693258d9c35a/EN_wp_LSM-Plus_Practical-Guide-of-Deconvolution.pdf
27. Zanier ER, Fumagalli S, Perego C, Pischiutta F, De Simoni MG. Shape descriptors of the "never resting" microglia in three different acute brain injury models in mice. *Intensive Care Med Exp*. 2015;3:7. https://doi.org/10.1186/s40635-015-0039-0
28. Aijima R, Wang B, Takao T, et al. The thermosensitive TRPV3 channel contributes to rapid wound healing in oral epithelia. *FASEB J*. 2015;29(1):182–192. https://doi.org/10.1096/fj.14-251314
29. Yamasaki R, Fujii T, Wang B, et al. Allergic inflammation leads to neuropathic pain via glial cell activation. *J Neurosci*. 2016;36(47):11929–11945. https://doi.org/10.1523/JNEUROSCI.1981-16.2016
30. Ito D, Imai Y, Ohsawa K, Nakajima K, Fukuuchi Y, Kohsaka S. Microglia-specific localisation of a novel calcium binding protein, Iba1. *Mol Brain Res*. 1998;57(1):1–9. https://doi.org/10.1016/s0169-328x(98)00040-0
31. Hanani M, Spray DC. Emerging importance of satellite glia in nervous system function and dysfunction. *Nat Rev Neurosci*. 2020;21(9):485–498. https://doi.org/10.1038/s41583-020-0333-z
32. Ji RR, Berta T, Nedergaard M. Glia and pain: is chronic pain a gliopathy? *Pain*. 2013;154(Suppl 1):S10–S28. https://doi.org/10.1016/j.pain.2013.06.022
33. Gouin O, L'Herondelle K, Lebonvallet N, et al. TRPV1 and TRPA1 in cutaneous neurogenic and chronic inflammation: pro-inflammatory response induced by their activation and their sensitization. *Protein Cell*. 2017;8(9):644–661. https://doi.org/10.1007/s13238-017-0395-5
34. Tan LL, Bornstein JC, Anderson CR. Distinct chemical classes of medium-sized transient receptor potential channel vanilloid 1-immunoreactive dorsal root ganglion neurons innervate the adult mouse jejunum and colon. *Neuroscience*. 2008;156(2):334–343. https://doi.org/10.1016/j.neuroscience.2008.06.071
35. De Logu F, Nassini R, Hegron A, et al. Schwann cell endosome CGRP signals elicit periorbital mechanical allodynia in mice. *Nat Commun*. 2022;13(1):646. https://doi.org/10.1038/s41467-022-28204-z
36. Millqvist E. TRPV1 and TRPM8 in treatment of chronic cough. *Pharmaceuticals (Basel)*. 2016;9(3):45. https://doi.org/10.3390/ph9030045
37. McGarvey LP, Butler CA, Stokesberry S, et al. Increased expression of bronchial epithelial transient receptor potential vanilloid 1 channels in patients with severe asthma. *J Allergy Clin Immunol*. 2014;133(3):704–712.e4. https://doi.org/10.1016/j.jaci.2013.09.016
38. Rehman R, Bhat YA, Panda L, Mabalirajan U. TRPV1 inhibition attenuates IL-13 mediated asthma features in mice by reducing airway epithelial injury. *Int Immunopharmacol*. 2013;15(3):597–605. https://doi.org/10.1016/j.intimp.2013.02.010
39. Cevikbas F, Wang X, Akiyama T, et al. A sensory neuron-expressed IL-31 receptor mediates T helper cell-dependent itch: involvement of TRPV1 and TRPA1. *J Allergy Clin Immunol*. 2014;133(2):448–460. https://doi.org/10.1016/j.jaci.2013.10.048
40. Meyer RA, Ringkamp M, Campbell JN, Raja SN. Peripheral mechanisms of cutaneous nociception. In: McMahon SB, Koltzenburg M, eds. *Wall and Melzack's Textbook of Pain*. 5th ed. Elsevier; 2006:3–34.
41. Wilzopolski J, Kietzmann M, Mishra SK, Stark H, Bäumer W, Rossbach K. TRPV1 and TRPA1 channels are both involved downstream of histamine-induced itch. *Biomolecules*. 2021;11(8):1166. https://doi.org/10.3390/biom11081166
42. von Buchholtz LJ, Ghitani N, Lam RM, Licholai JA, Chesler AT, Ryba NJP. Decoding cellular mechanisms for mechanosensory discrimination. *Neuron*. 2021;109(2):285–298.e5. https://doi.org/10.1016/j.neuron.2020.10.028
43. Murthy SE, Loud MC, Daou I, et al. The mechanosensitive ion channel Piezo2 mediates sensitivity to mechanical pain in mice. *Sci Transl Med*. 2018;10(462), eaat9897. https://doi.org/10.1126/scitranslmed.aat9897
44. Szczot M, Liljencrantz J, Ghitani N, et al. PIEZO2 mediates injury-induced tactile pain in mice and humans. *Sci Transl Med*. 2018;10(462), eaat9892. https://doi.org/10.1126/scitranslmed.aat9892
45. Megat S, Ray PR, Tavares-Ferreira D, et al. Differences between dorsal root and trigeminal ganglion nociceptors in mice revealed by translational profiling. *J Neurosci*. 2019;39(35):6829–6847. https://doi.org/10.1523/JNEUROSCI.2663-18.2019
46. Ji RR, Donnelly CR, Nedergaard M. Astrocytes in chronic pain and itch. *Nat Rev Neurosci*. 2019;20(11):667–685. https://doi.org/10.1038/s41583-019-0218-1
47. Stence N, Waite M, Dailey ME. Dynamics of microglial activation: a confocal time-lapse analysis in hippocampal slices. *Glia*. 2001;33(3):256–266. https://doi.org/10.1002/1098-1136(200103)33:3<256::AID-GLIA1024>3.0.CO;2-J
48. Schwerin SC, Chatterjee M, Imam-Fulani AO, et al. Progression of histopathological and behavioral abnormalities following mild traumatic brain injury in the male ferret. *J Neurosci Res*. 2018;96(4):556–572. https://doi.org/10.1002/jnr.24218
49. Kelkar M, Bohec P, Charras G. Mechanics of the cellular actin cortex: from signalling to shape change. *Curr Opin Cell Biol*. 2020;66:69–78. https://doi.org/10.1016/j.ceb.2020.05.008
50. Feldman-Goriachnik R, Hanani M. How do neurons in sensory ganglia communicate with satellite glial cells? *Brain Res*. 2021;1760, 147384. https://doi.org/10.1016/j.brainres.2021.147384
51. Rosas-Hernández R, Bastián Y, Juárez Tello AJ, et al. AMPA receptors modulate the reorganization of F-actin in Bergmann glia cells through the activation of RhoA. *J Neurochem*. 2019;149(2):242–254. https://doi.org/10.1111/jnc.14658
52. Lemes JBP, de Campos Lima T, Santos DO, et al. Participation of satellite glial cells of the dorsal root ganglia in acute nociception. *Neurosci Lett*. 2018;676:8–12. https://doi.org/10.1016/j.neulet.2018.04.003
53. Spray DC, Iglesias R, Shraer N, et al. Gap junction mediated signaling between satellite glia and neurons in trigeminal ganglia. *Glia*. 2019;67(5):791–801. https://doi.org/10.1002/glia.23554
54. Furuyashiki T, Arakawa Y, Takemoto-Kimura S, Bito H, Narumiya S. Multiple spatiotemporal modes of actin reorganization by NMDA receptors and voltage-gated Ca^{2+} channels. *Proc Natl Acad Sci U S A*. 2002;99(22):14458–14463. https://doi.org/10.1073/pnas.212148999
55. Zhang Z, Kindrat AN, Sharif-Naeini R, Bourque CW. Actin filaments mediate mechanical gating during osmosensory transduction in rat supraoptic nucleus neurons. *J Neurosci*. 2007;27(15):4008–4013. https://doi.org/10.1523/JNEUROSCI.3278-06.2007
56. Omari SA, Adams MJ, Geraghty DP. TRPV1 channels in immune cells and hematological malignancies. *Adv Pharmacol*. 2017;79:173–198. https://doi.org/10.1016/bs.apha.2017.01.002
57. Choi JY, Lee HY, Hur J, et al. TRPV1 blocking alleviates airway inflammation and remodeling in a chronic asthma murine model. *Allergy Asthma Immunol Res*. 2018;10(3):216–224. https://doi.org/10.4168/aair.2018.10.3.216
58. Khalid S, Murdoch R, Newlands A, et al. Transient receptor potential vanilloid 1 (TRPV1) antagonism in patients with refractory chronic cough: a double-blind randomized controlled trial. *J Allergy Clin Immunol*. 2014;134(1):56–62. https://doi.org/10.1016/j.jaci.2014.01.038
59. Belvisi MG, Birrell MA, Wortley MA, et al. XEN-D0501, a novel transient receptor potential vanilloid 1 antagonist, does not reduce cough in refractory cough patients. *Am J Respir Crit Care Med*. 2017;196(10):1255–1263. https://doi.org/10.1164/rccm.201704-0769OC
60. Srour J, Bengel J, Linden T, et al. Efficacy of a skin care cream with TRPV1 inhibitor 4-t-butylcyclohexanol in the topical therapy of perioral dermatitis. *J Cosmet Dermatol*. 2020;19(6):1409–1414. https://doi.org/10.1111/jocd.13175